TASK QUARTERLY 9 No 1, 65–79

FLOW CHARATERISTICS OF A LOW NO_x EMISSION BURNER

DARIUSZ KARDAŚ AND SŁAWOMIR GOLEC

Institute of Fluid Flow Machinery,
Polish Academy of Sciences,
Fiszera 14, 80-952 Gdansk, Poland
{dk, sgolec}@imp.gda.pl

(Received 7 May 2004)

Abstract: Recent technological changes in the Polish power industry have created opportunities for reducing NO_x and CO emissions, but – at the same time – created another operation problem: sulphur corossion of boilers' rear water-wall. This has been the motivation for performing a detailed study of the air flow and pulverized coal transport in low-NO_x burners. A measuring stand was built inside a real medium power OP-230 boiler equipped with a low-NO_x burner to measure the velocity field at the burner's outlet and to prepare experimental characteristics of the burner. To extend the description, a numerical model of the burner was constructed and numerical calculations were executed by means of the Fluent program. Numerically calculated velocity profiles were compared with the results of measurements. Further investigations of the low NO_x burner included the flow of the air-pulverized coal mixture. The measured concentration of the coal dust was compared with numerically predicted distribution of particles. Both the measurements and the calculations have shown a highly non-uniform concentration of particles at the burner outlet. The obtained results have been helpful in formulating recommendations to improve burner geometry.

Keywords: combustion, pulverised coal burner, NO_x, SO_2, environmental pollution, sulphur corrosion

1. Introduction

There have been many technological changes in the Polish power industry in the recent years, but coal remains a dominating source of energy and its position will certainly not be shaken in the next several years. It results both from economic reasons and from the imperative of energetic security of the country. The cost of electricity obtained from coal is half that of electricity produced from natural gas. According to a DOE report [1], natural gas fuel costs are expected to rise whereas those of coal will decline. Moreover, the question of permanent and undisturbed access to energy sources is becoming more and more important nowadays. The persistent instability in the former Soviet Union countries and in the Middle East shows that excessive reliance on foreign oil is a costly proposition – in political, military and economic terms. Fortunately, Poland has plentiful domestic resources of coal to generate electricity – and new technologies allow to meet the growing demand for electricity more efficiently.

However, coal combustion is inseparably associated with environmental pollution. The major pollutants produced in the combustion proccess are unburned and partially burned hydrocarbons, carbon monoxide, sulfur oxides, nitrogen oxides, and particulate matter in various forms. All these compounds affect the environment and human health in many ways, the most important of which are:

- potential increase of sickness and mortality of the population,
- altered properties of the atmosphere and precipitation,
- worsened conditions of vegetation,
- soiling and deterioration of materials.

Because of the large number of uncontrolled variables, it is not easy to explicitly measure the effect of pollution on human health. However it is well known that carbon-based particles may contain adsorbed carcinogens. It is also observed that pollutants can aggravate pre-existing respiratory ailments. The occurence of acute and chronic bronchitis can be correlated with SO_2 and particulate matter.

Altered properties of the atmosphere affecting local areas include: reducing visibility, increasing fog formation and precipitation, altering temperature and wind distributions, reducing solar radiation. On a larger scale, greenhouse gases may alter global climates.

Lakes and susceptible soils are affected by acid rain produced from SO_x and NO_x emissions. Vegetation is harmed by the action of phytotoxicants SO_2, peroxyacetyl nitrate (PAN), C_2H_4 and others.

Particulate matter, especially that containing sulfur, corrodes paint, masonry and electrical contacts, while ozone severely deteriorates rubber.

The huge volume of combusted coal and environmental pollution caused by flue gases have resulted in a growing interest in the improvement of the coal combustion technology. In order to reduce the pollution, Poland, like other industrialized countries, has adopted stringent emission standards and implemented emission control. In the early nineties the power industry made a great organizational and financial effort to reduce the emission of nitric oxides and carbon monoxide. It was achieved in various forms, dependening on the individual energy producer. Air gradation has been applied in certain instalations, whereas others employed low-emission burners with air redistribution. These two types of rebuilding required only a slight modernization of air ducts and met the environmental standards close enough. Moreover, these solutions are relatively cheap.

Like many other power plants, the Heat and Power Plant 'Wybrzeże' in Gdansk took it upon themselves to modernize most of their boilers. A general overhaul of the boilers was performed in 1994.

In the case of the OP-230 boiler, with tight screening of the burning chamber with natural circulation (boiler No. 10), the modernization mainly consisted in replacing swirl-type burners with low-emission units manufactured by Babcock Energy Ltd. and in admitting additional volume of air to the combustion chamber via OFA nozzles located in front of and behind the water wall. A sketch of the side view of the boiler with eight burners and six small OFA nozzles is shown in Figure 1.

The boiler is equipped with a three-stage steam superheater, a water heater, and two rotating air heaters. It is supplied by four mills, three of them in continuous

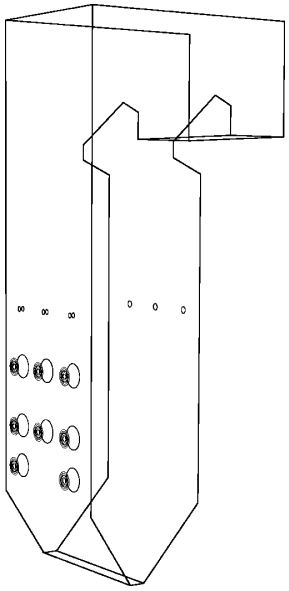

Figure 1. Burners and OFA nozzles' configuration in the OP-230 boiler

operation and the fourth kept in reserve. Each mill feeds two burners, so the fuel is injected by six burners. The burners are located on the boiler's front wall at a distance of 2.5 m from each other.

After the modernization, the boiler was in operation for 27 thousand hours, when its rear water wall was damaged in the spring of 1998 [2]. A tube was torn apart at the level of 14 m – the top row of burners. Thickness measurements of the tube walls in the vicinity of the damaged part made after the failure, revealed a reduction in thickness from 5 mm, which was the nominal value, down to a minimum thickness of 1.4 mm. The thickness defect was recorded along half-perimeter from the furnace side, 'from fin to fin', the minimum thickness being located at the top of the tube.

Chemical analyses confirmed unmistakably the correct ferrite-and-bainite structure of the tube's steel, and its low degradation level, recorded both from the side of the furnace gas and that of the furnace lining. An increased concentration of sulphur was observed in the deposits taken from tubes along with increased contents of oxygen, potassium, magnesium and calcium, which testified to a high concentration of sulphides. High contents of sulphur in the layer and uniform material decrement in the tubes testified to sulphide corrosion of the boiler's rear water wall.

Measurements of the pipe's thickness have shown that the rate of corrosion in this boiler was equal to 0.7–1 mm per year, while it had been 10 times lower before the modernization.

It thus came out that the new installation significantly reduced NO_x emission, but at the same time caused serious damage to the boiler, and remained a threat to its faultless exploitation. A detailed study of combustion proccess in the new low-emission burner became necessary also for technological reasons.

2. Burner characteritics

The geometry of the low-NO_x emission swirl burner manufactured by Babcock Energy (Figure 2) is more complex than that of a standard swirl burner. The air flowing into the combustion chamber is divided into core, primary, secondary and tertiary. The secondary air of the standard low-NO_x burners is divided into secondary and tertiary air. In this way an additonal possibility of combustion process control is achieved, through diversification of the air fluxes at the outlet. The angles of vanes mounted in the second and third air channels are different and adjustable, providing opportunities for changing the length of the swirl jet.

Figure 2. A Babcock Energy burner during measurements of the velocity components in the OP-230 boiler No. 10, Heat and Power Plant in Gdansk

Series of measurements were carried out to prepare the experimental characteristics of the burner and determine the velocity field at the outlet [3]. During the experiment the coal mill was merely ventilated and no coal was flowing through the burner, while in the normal operation of the boiler pulverized coal is mixed with primary air. The measuring probe was mounted on a system of movable guiding rails located co-axially with the burner (Figures 2 and 3). Because of a high level of dust in the chamber, a strenghtened Dantec fibre-split thermo-anemometer probe was used. The probe made it possible to measure the axial and the tangential velocity components, as well as their fluctuations. The measurements were realized in cross-sections 0, I, II, III (Figure 3). Cross-section 0 was situated at a distance of 1 cm from the burner's outlet, cross-section I – 20 cm, cross-section II – 66 cm, and cross-section III – 91 cm from the outlet of the burner.

The output of primary and secondary air was measured independently and recorded in the control room of the power unit. Moreover, it was possible to control the swirl of secondary air using a special swirler situated in the secondary air space inside the burner. Approximate conditions of burner work are given in Table 1.

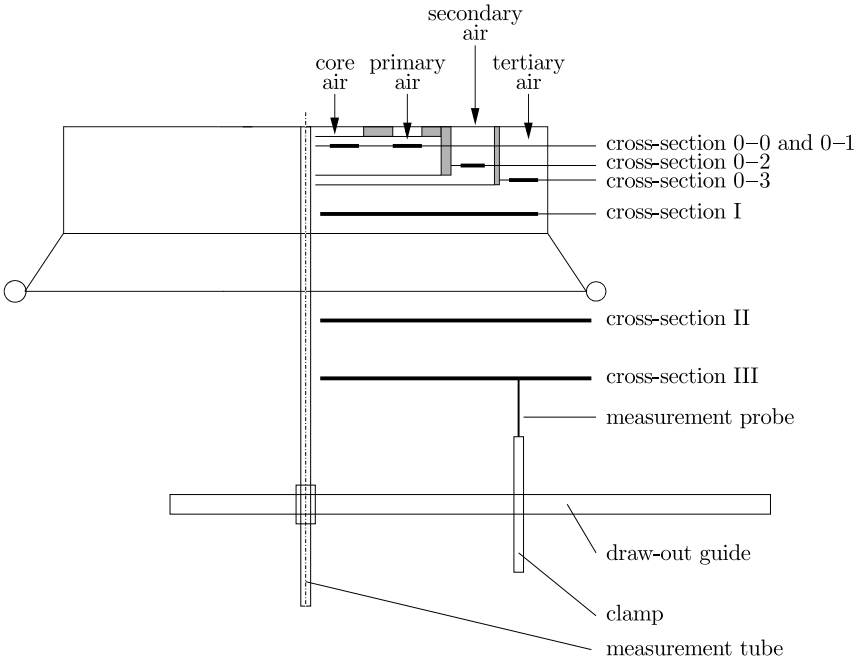

Figure 3. Measurement cross-sections at the outlet of the Babcock Energy burner

Table 1. Measurement conditions for the Babcock Energy burner

	Flow volume	Temperature
Core air	2800m^3/h	22°C
Primary air	7500m^3/h	45°C
Secondary air	17000m^3/h	22°C

Properties of the swirl flow can be correctly described by the swirl number, according to the following formula:

$$S = \frac{2}{d}\frac{G_\theta}{G_x}, \tag{1}$$

where d is the stream diameter, G_θ is the tangential momentum component and G_x is the axial momentum component, both given by the following formulas:

$$G_\theta = \int_0^\infty (\rho UW + \rho u'w')r^2\,dr, \tag{2}$$

$$G_x = \int_0^\infty \left(\rho U^2 + \rho u'^2 + (p - p_\infty)\right) r dr, \tag{3}$$

where U and W are the axial and circumferential components of the air stream, while u' and w' are fluctuations of axial and circumferential components of velocity, respectively, ρ is density, p and p_∞ stand for the actual value of pressure and the value of pressure at infinity.

In the case of incompressible flow, disregarding the influence of fluctuations of velocities u' and w' simplifies the formula considerably:

$$S = \frac{2}{d} \frac{\int_0^\infty UW r^2 dr}{\int_0^\infty U^2 r dr}. \tag{4}$$

On the basis of the measurements, a square-mean approximation of the swirl number was computed in relation to the swirl vane used and diaphragm settings. Their influence on the averaged S is relatively low, and the swirl number curve as a function of diaphragm setting and the swirl vane varies within the range of 0.47–0.69.

3. Measurements versus numerics

As mentioned above, the experimental characteristics of the burner were developed in several cross-sections only. To extend the description of the burner to the whole of the combustion chamber, a numerical model of the burner was constructed (Figures 4, 5 and 8) with a part of the combustion chamber of the size $4\,\mathrm{m} \times 4\,\mathrm{m} \times 6\,\mathrm{m}$. The geometry of the burner was simplified. It was assumed that some of the blades were plane, while in practice they were half-rounded, and the thickness of most of the burner walls and blades was assumed to equal zero. However, the inner walls and blades were included, as shown in Figures 9, 14 and 15. Because of the complicated geometry, different types of cells were used. A majority of the burner cells was of the tetrahedral type whereas the combustion chamber consisted of hexahedral cells. For most of the numerical tests the number of cells did not exceed 1000000.

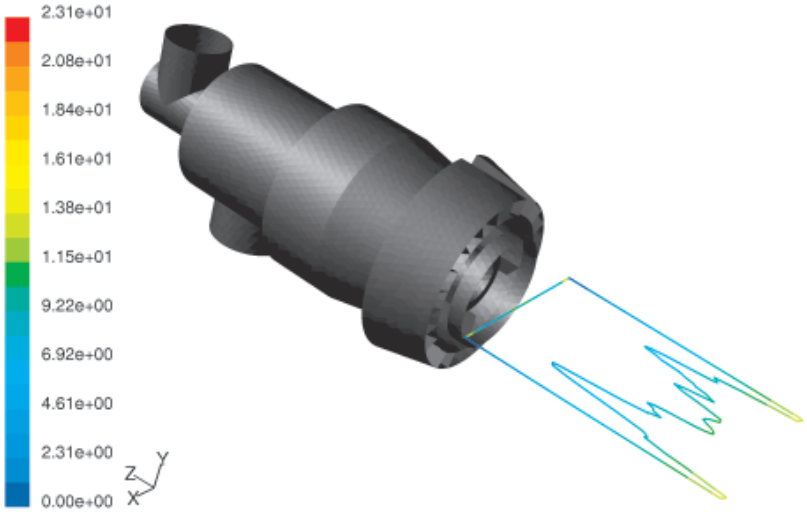

Figure 4. Geometry of the numerical model of the burner and the profile of velocity magnitude [m/s] at a distance of 20 cm from the outlet

All computations concerning the flow of air and the air-pulverised coal mixture through the burner were carried out by means of Fluent [4].

Table 2. Air boundary conditions for the numerical calculations of the Babcock Energy burner

	Mass flow	Temperature
Core air	0.75kg/s	293K
Primary air	1.7kg/s	318K
Secondary air	1.2kg/s	293K
Tertiary air	3.45kg/s	293K

The numerical air boundary conditions were based on the measurements and are presented in the Table 2.

The numerical calculations were executed using a k-ε turbulence model of very good convergence, and the RNG k-ε model, which yielded a solution with the residuum exceeding 10^{-3}.

Selected results of these calculations are shown in Figures 4–9. Figure 4 shows a view of the burner in the horizontal plane, along with the velocity profile at a distance of 20cm from the burner outlet. Looking from the left, the inlets of core and primary air are visible. One can also see covered inlets of secondary and tertiary air. The velocity profile in the plane marked in the picture, is not symmetric with respect to the burner axis. This asymmetry is insignificant and results from the burner's construction.

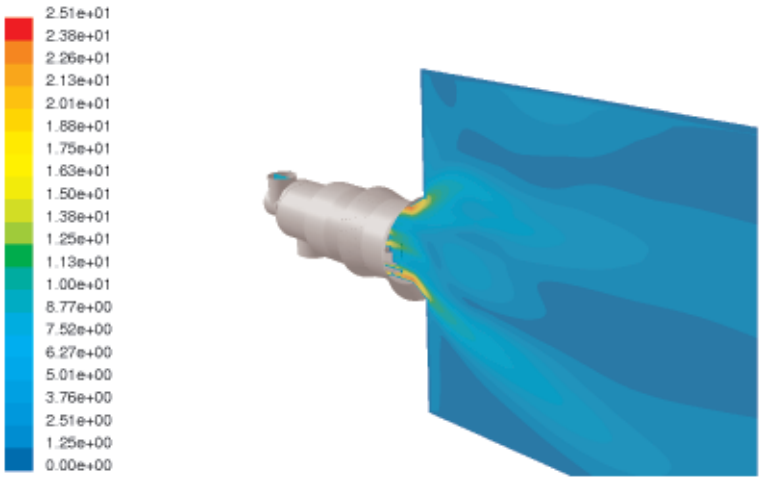

Figure 5. Velocity magnitude [m/s] in the cross-section along the burner axis

Figure 5 shows, in an axonometric projection, velocity magnitude contours in the vertical plane along the burner's axis. The edges of the inner walls and burner blades are also marked, along with a fragment of the modeled combustion chamber. The tangential velocity component, in the intersection along the burner axis in the vertical plane and the whole modeled combustion chamber, are presented in Figure 6.

Velocity modulus contours at the outlet of the burner are shown in Figure 7. One can see the influence of four separating blades and tertiary air blades on velocity. An assymetry of the burner's work can be observed as well.

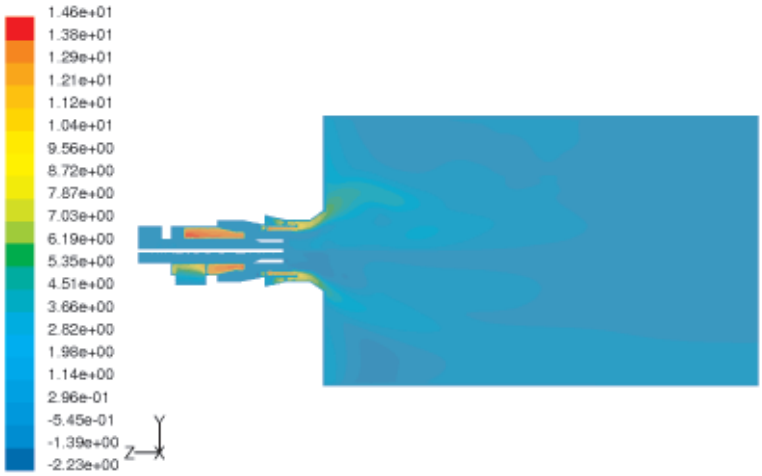

Figure 6. The tangential velocity component [m/s] in the cross-section along the burner

Figure 8 shows the streamlines. Inner blades of the burner and selected fragments of walls separating particular streams of air are also shown in the figure. One can easily observe the configuration of streamlines inside the burner and inside the combustion chamber. It is noteworthy that the air blown into the numerically modelled chamber has the form of a slightly expanding stream.

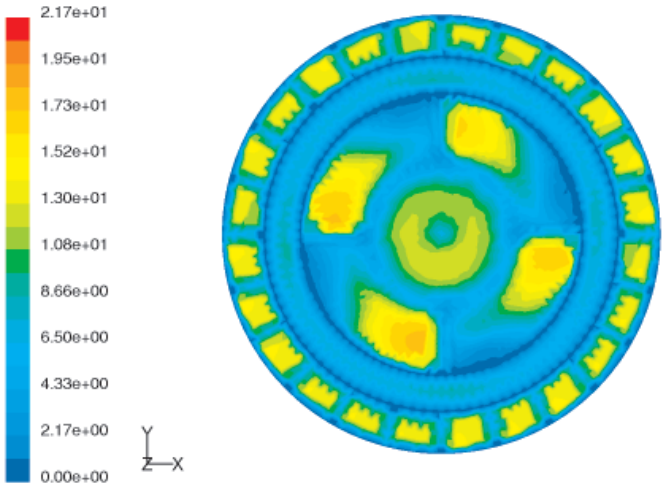

Figure 7. Velocity modulus in the crosswise direction (with respect to the axis of the burner) at the burner outlet

Velocity profiles, calculated numerically, are compared with the results of measurements in Figure 9. The figure consists of eight plots, arranged in two columns and four rows. The first and second columns show the axial and circumferential components of the velocity vector, respectively. The rows correspond to cross-sections 0, I, II and III. In each plot, the X axis represents radius r [m] (measured from the axis of the burner), while the Y axis represents a component of the velocity vector [m/s].

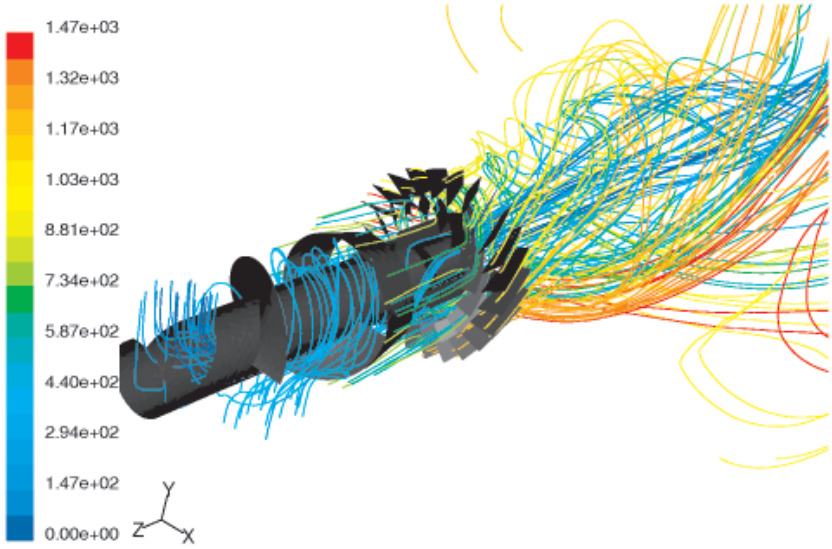

Figure 8. Streamlines with marked internal blades and the wall separating primary and secondary air; the beginning fragment of the wall separating the second from the third air flow is marked

The solid line corresponds to numerically computed values, while the dots mark the measurements data.

The least compatibility between the measurements and the calculations is observed for core air, particularly in cross-section I, for the axial component (see Figure 9). This discrepancy may be due to the presence of the leading pipe along the burner axis. The pipe was neglected in the numerical model used for the calculations.

Further from the burner outlet (cross-sections II and III) the consistency between the calculated and measured profiles of the axial and circumferential components is better.

There is qualitatively good consistency of calculations and measurements for primary air, particularly in cross-section 0. In other cross-sections the numerical solution is similar to most of the measurements of velocity vector components. The least consistency is observed in cross-section I. It may result from the different shapes of primary air blades (separators).

There is qualitatively good agreement for secondary air in cross-section 0, while further from the burner outlet, *i.e.* in cross-section I, one can observe excessive values of the axial component of the velocity vector (Figure 9). However, the difference is insignificant. In cross-section II, there is good consistency of the axial and tangential components of the velocity vector. These discrepancies were undoubtedly caused by the simplification of the burner geometry.

Other inconsistencies could have resulted from inaccuracies of measurement. While the real flow was fully three-dimensional, the probes used in the measurements were appropriate for 2D flows, which increased the measurement error. One should also bear in mind the differences in the temperature of core and primary air, and between primary (45°C) and secondary air (22°C), which were assumed to be equal.

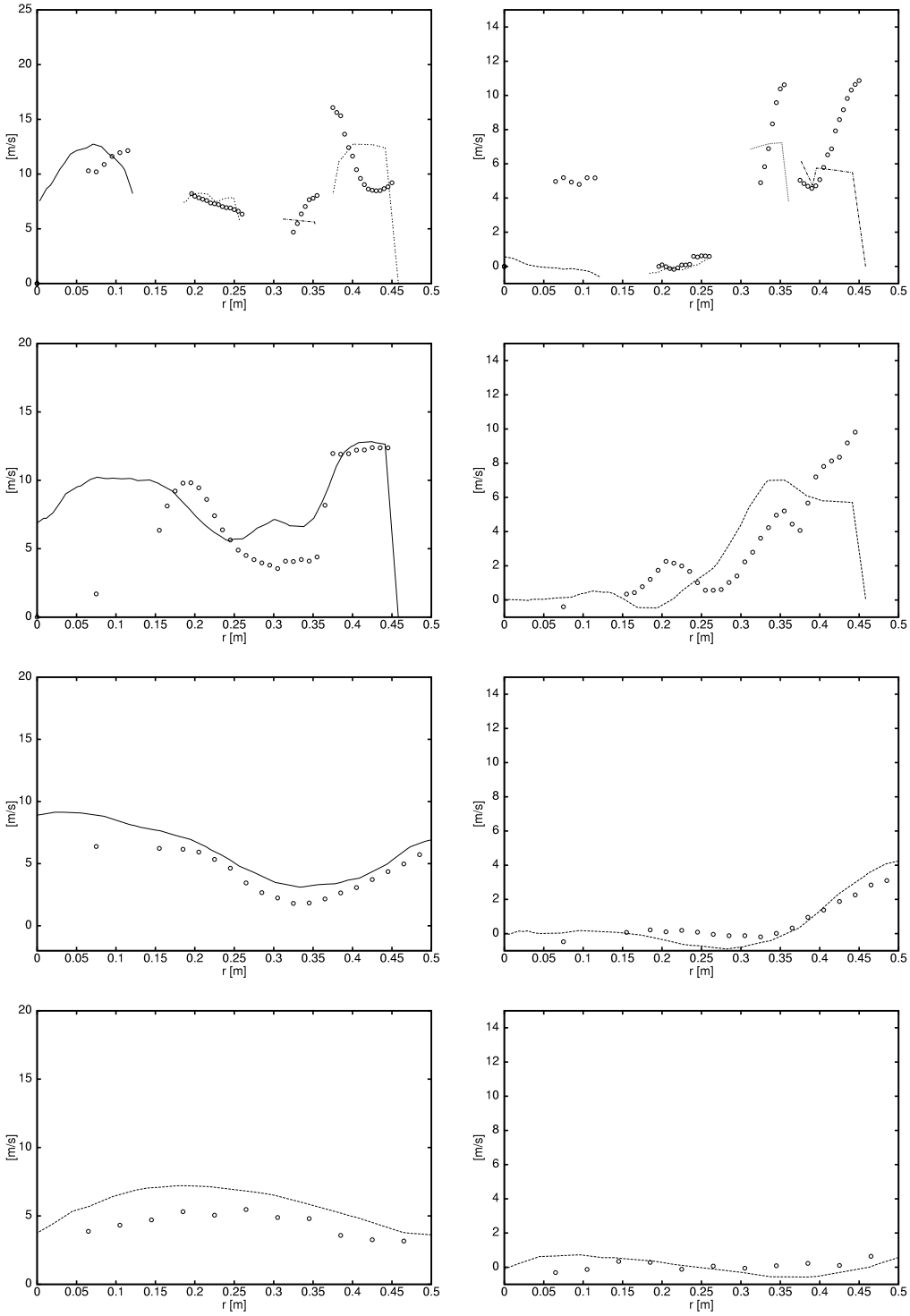

Figure 9. Velocity component cross-sections 0, I, II, III. The first and second columns present the axial and radial components, respectively. Measurement data are marked with dots, numerical results – with lines

4. Flow of the air-pulverized coal mixture

The low-NO_x emission swirl burner is in practice supplied with pulverized coal of particle diameters between 30μm and 150μm. The size of particles mostly depends on the construction and operating conditions of the coal mill and on the properties of the coal. After entering the burner, the pulverized coal is swirled by a screw blade, as shown in Figures 8, 14 and 15. The swirled air-coal mixture contacts four separating blades situated parallelly to the burner axis (Figures 2, 14 and 15). These blades are intended to increase the concentration of pulverized coal in their vicinity and thus reduce the level of mixing of coal particles with air. Along with low excess air, this solution should result in decreased combustion rates and NO_x emission.

To investigate the operation of the low-NO_x emission burner, a model of the burner was built for Rafako Ltd. [5]. Then an experimental stand was prepared to examine the model of the burner. The main purpose was to determine the concentration of pulverized coal at the burner outlet, along its perimeter. The experimental stand (Figure 10) consisted of a vertical inlet pipe, the burner model, a measuring head and measuring probes. The air and pulverized coal mixture was transported in the pipe from the coal mill to the measuring chamber. Thick fractions were separated in the auxiliary coal-powder vessel, whereas the rest of the coal-powder left the chamber through the outlet. At the outlet part of the chamber two probes were mounted to take samples. The measuring points were uniformly distributed along the burner perimeter (Figure 11). Points 12, 3, 6 and 9 were located on the levels of four separating blades. The inlet pipe was 6m long. Contrary to the real pipeline system with short pipes and numerous elbows, in the experiment the distribution of coal-powder particles at the inlet of the burner was almost uniform. Measurements were realized for two measuring circles of diameters, d_1 =131mm and d_2 =105mm. The sieve analysis of the pulverized coal was performed (Table 3) in a pneumatic sieving device, where the dimensions of pulverized coal left on the sieves were determined as equal to 60μm, 88μm, 120μm. The transporting air temperature in front of the separator was kept within the range of 100–120°C.

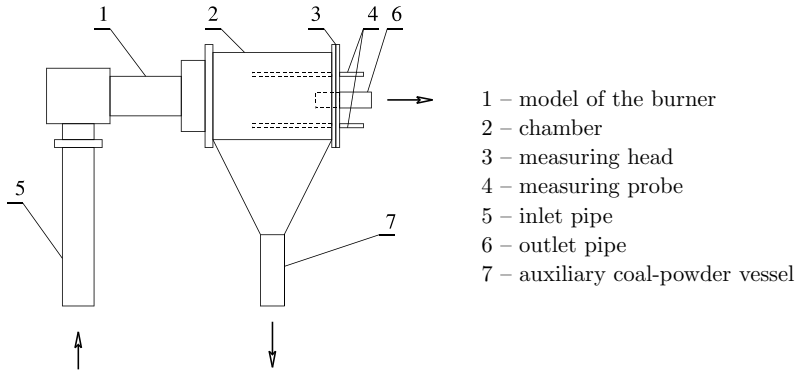

Figure 10. Scheme of the experimental stand

The measurement results are presented in Table 4. It can be clearly seen that the pulverized coal's concentration is far from uniform. The coal density ratio at points

Table 3. Sieve analysis of the coal used in the experimental stand. Sieve meshes in μm

Sieve mesh	%
R_{60}	27.6
R_{88}	12.7
R_{120}	4.2

6 and 12 is about 3.6, and about 4.4 at points 6 and 3. This means that most of the coal stream flows in the form of two thick tails around points 6 and 9, the stream from point 6 being dominant.

Table 4. Measurement results of the coal-powder concentration distribution at the outlet of the burner model

Point number	Coal concentration at distance d_1 [kg/m^3]	Coal concentration at distance d_2 [kg/m^3]
1	0.29	0.22
2	0.14	0.17
3	0.21	0.43
4	0.16	0.19
5	0.15	0.31
6	0.92	1.11
7	0.36	0.55
8	0.24	0.45
9	0.46	0.64
10	0.22	0.34
11	0.20	0.25
12	0.25	0.43

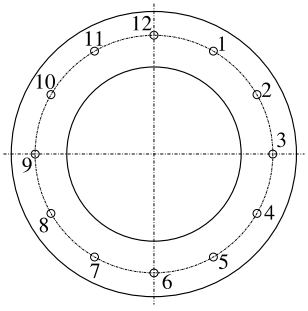

Figure 11. The location of measuring points at the burner outlet

Simultaneously with the experiment, numerical calculations of coal particle flow in the burner and the combustion chamber were carried out. As mentioned above, the geometry of the burner was simplified, though it was still relatively complex. A good example of the complexity of the numerical model of the burner is the number of surfaces, which exeeds 120. The thickness of all blades and most of the walls was

assumed to equal zero. The Lagrangian approach was used to model the pulverized coal flow. The interaction between the calculated air velocity field and that of the discrete phase was included. The k-ε model of turbulence was applied. In the numerical experiment the burner was supplied with air and pulverized coal uniformly distributed at the inlet. The powder consisted of particles of diameters between $30\,\mu$m and $150\,\mu$m, and the mass stream of the coal-powder was equal to 41.8g/s.

Figure 12 shows the distribution of pulverized coal's concentration at the burner outlet at twelve measuring points. The solid line corresponds to the numerically calculated values, whereas the dashed lines show the values measured during the experiment. The calculations and measurements are consistent in that most of the coal-powder is concentrated close to the low separating blade, which corresponds to point 6 in Figure 11. The two side separating blades (points 3 and 9) capture less pulverized coal. The least of it is concentrated near the upper separating blade (point 12). Similiar conclusions can be drawn from Figure 13. It shows an axonometric view of the coal's constant concentration zones along the outer walls. A wide area of concentration of the dispersed phase can be seen in the bottom part of the burner outlet, especially around point 9. This figure indicates four places where the dispersed phase is dense, while the rest of the outlet is free of coal powder. Strong influence of the four separating blades on the concentration of pulverized coal at the burner outlet can be observed.

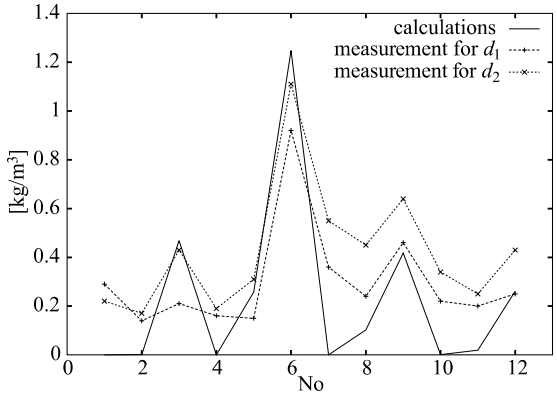

Figure 12. Distribution of coal powder concentration at the burner outlet

The non-uniformity of the coal distribution begins more upwind, as can be noticed in Figures 14 and 15. Indeed, the screw blade has a large impact on the burner's work. The figures show path lines of pulverized coal's particles. It can also be observed that the screw blade can succesfully swirl the flow. However, the cooperation of the screw blade with the four separating blades is not correct and results in non-uniform distribution of pulverized coal on particular separating blades. One can also observe why the lowest separating blade captures pulverized coal particles. This effect was measured and presented in Figure 12, where areas of constant concentration of coal in the burner can be seen.

The discrepancy between the calculations and the measurements can be explained by differences between the real burner geometry and that assumed for the

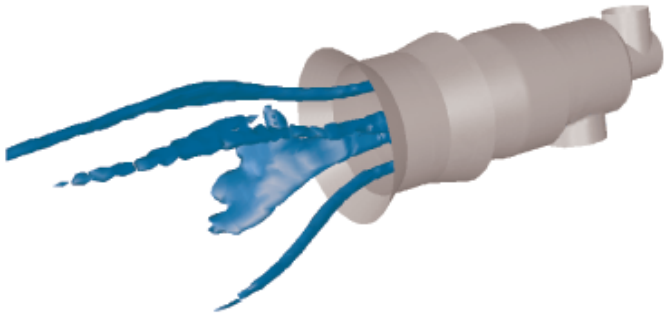

Figure 13. Constant concentration zones of coal particles at the burner outlet

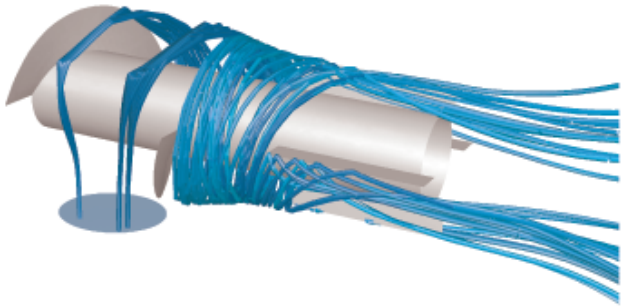

Figure 14. Path lines of pulverized coal particles, left-hand side view

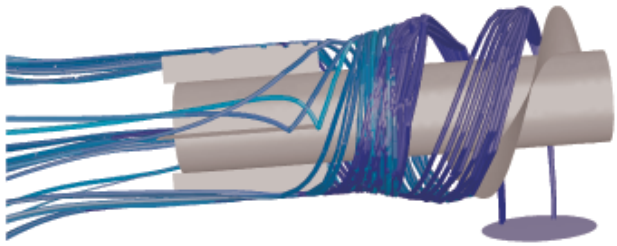

Figure 15. Path lines of pulverized coal particles, right-hand side view

calculations. It was also assumed that the pulverized coal distribution at the burner inlet is uniform, which is not true in practice.

Comparing the results of the experiment and the calculations, one can note the correctness of the adopted calculation method and the assumed simplifications.

Non-uniform distribution of the coal dust on the perimeter causes different combustion conditions for different coal tails. A jet of high concentration of coal generates a high level of CO in the vicinity of the rear wall of the boiler, a source of sulphur corrosion. As this effect is highly undesirable, modifications are necessary to achieve more homogenous fuel distribution at the burner outlet. The burner needs an alteration in the form of an additional screw blade to direct more coal particles into the upper part of the burner outlet. In a real pipe system, even an additional screw blade may not be sufficient in the case of high local concentration caused by short pipes and elbows. In such a situation, a reduction in the flow area will be necessary together with the use of a breaking element.

5. Conclusions

Measurements and numerical calculations presented above allow the basic characteristics of the low-NO_x burner to be defined. First of them is a relatively low swirl number. The swirl is very weak at the core and primary air areas and increases in secondary and tertiary air areas. Thus, it can be concluded that primary air transports coal powder deep into the combustion chamber. More intensive mixing of coal powder and air takes place in the secondary air volume. The other characteristic feature of the burner is highly non-uniform coal-powder distribution at the burner perimeter. The highest coal-powder concentration is observed in its lower part, near the separating blade. The non-uniform coal-powder distribution is transported into the combustion chamber, causing a locally high coal concentration, which results in high a concentration of CO. This type of combustion may lead to corrosion of a boiler's rear water wall, which took place at the Wybrzeze Heat and Power Plant. This non-uniformity can be reduced by means of an additional screw blade.

Acknowledgements

The majority of calculations were made at the Academic Computer Center TASK Gdansk.

References

[1] http://www.eia.doe.gov/oiaf/aeo/electricity.html
[2] Kardaś D, Michalski M and Janczewski J 2000 *5th European Conf. on Industrial Furnances and Boilers*, Espinho-Porto
[3] Wierciński Z, Kardaś D, Topolski J and Kaiser M 1998 *Air Characteristics of a Babcock Burner in Power Plant in Gdansk*, IFFM Report No. 263/98 (in Polish)
[4] *Fluent User's Guide, Release 6.0*, Fluent Incorporated, 2003
[5] Wala T 2001 *private communication*